

Control of air pressure inside an inflatable textile pocket of an active backrest cushion

Adeel MEHMOOD, Rodolfo ORJUELA and Michel BASSET

*Modélisation Intelligence Processus Systèmes (MIPS) laboratory, EA 2332
Université de Haute-Alsace 12 rue des frères lumière
F-68093 Mulhouse cedex, France.*

E-mail: (adeel.mehmood, rodolfo.orjuela, michel.basset)@uha.fr

Abstract: The objective of this paper is to propose a control strategy of air pressure inside an Inflatable Textile Pocket (ITP) in order to design an adjustable seat backrest for drivers comfort. For the said purpose, firstly a brief model of an Electro-pneumatic Pressure Converter (EPC) is presented along with the pressure dynamics inside an IFP. This nonlinear model is then linearized around an operating point and a control synthesis is performed using the classical linear control theory. The obtained PID controller is implemented on a developed experimental test bench. Furthermore, a comparative analysis, between the feedback responses obtained with the help of the proposed control and an industrial pressure regulator, is also performed to show the effectiveness of the proposed controller.

1. INTRODUCTION

The idea proposed in this work to reduce driver's discomfort is to replace classical seat by an adjustable and inflatable seat cushion. The proposed idea is implemented by the means of an active seat system with the unique feature of getting configured according to the drivers morphology, which in turns help the driver to encounter difficult driving situations. The major components of this system are: a pressure supply, an inflatable textile pockets and an Electro-pneumatic Pressure Converter (EPC) device as described in Fig. 1.

The exiting inflatable systems being used in the automotive industry are the inflatable seat belts, the inflatable bumpers and the steering airbags (Chawla et al., 2005; Rangnath, 2009). All these materials use stretchable polymer material which can be easily torn off. Also each component being made by mold requires a separate mold. In the proposed developed active seat system, these classic inflatable pockets are replaced by Inflatable Textile fabric Pockets (ITP) in order to reduce the dubiousness of design. The ITP employed in this work are made by textile fibres. Studies have shown that these textile pockets are better than classical inflatable systems with respect to strength and different complex structures could be made with the help of computer aided designs and without any dependence of mold (Tulemat, 2007; Alali, 2008).

The ITP is pressurized through a pressure converter which is a proportional servo valve. It consists of a plunger which may attain different positions that are linearly proportional to the applied voltage signal (see for example (Rao and Bone, 2008) and (Wickramatunge and Leephakpreeda, 2013)). Modeling of the proportional valve considered in this study has already been discussed in the literature (Olaby et al., 2005; Gulati and Barth,

2007; Zilic et al., 2009; Zhang et al., 2013). However, dynamic behavior of its spool valve changes with each mark and application. Therefore, it has to be considered, here, for dynamic analysis of pressure. The spring action on the solenoid based spool valve allows it to attain different pressure values inside the ITP. Physical modeling of the pressure regulator has been addressed in the literature (Taghizadeh et al., 2009; Wang et al., 2007). However, its application to control an inflatable seat cushion was not addressed to the best of authors' knowledge. The pressure inside these ITPs depends on flow of air through the EPC which is modeled by using orifice flow equations (Heywood, 1988). In this work, a nonlinear model of inflatable seat system, which includes the EPC and the ITP, is presented and linearized around an operating point for the control synthesis.

The majority of the control process in the world are operated by the Proportional-Integral-Derivative (PID) controllers. It has been reported that about 90 % of the industrial process are based on PID controllers (Bialkowski, 1996). Similar statistics hold in the motion control and aerospace industry (Silva et al., 2002). However, a PID controller is not the only solution because we may experience limit cycles, with PID control, in presences of nonlinearities such as friction (Canudas de Wit et al., 1995). In this paper, we have implemented a PID controller on the experimental test bench. This controller will be employed in the future to compare its performance with more sophisticated control techniques, such as, the sliding mode control and the backstepping control Smaoui et al. (2007). The tracking performances obtained with the help of the integrated modelling/PID controller are compared with the performance of an industrial pressure regulator. The proposed controller offers better transient and steady state performances.

The paper is organized as follows. In section 2, a nonlinear model of the pneumatic pressure converter is presented along with pressure dynamics inside an Inflatable Textile Pocket (ITP). In section 3, The nonlinear model is linearized around

* This work is sponsored by the regional project ERGOFLUX [CONNECTUS-OSEO].

an operating point to design a PID controller. The experimental bench is presented in section 4 and tests are performed for two reference trajectories. Section 5 concludes the article.

2. SYSTEM MODELING

The Inflatable Textile Pocket (ITP) are used to obtain an active seat cushion (see Fig. 1). The whole system consists of a compressor, the EPC and an inflatable seat backrest which contains more than one pocket. Each pocket can sustain an absolute pressure up to 2Bar. The EPC is a proportional servo valve which regulates the pressure in the active seat system.

In this section, modeling of the two main parts of the system i.e. the pressure converter and the Inflatable Textile Pocket is discussed. The pneumatic lines joining all sub parts of the inflatable seat have short length. Therefore, the attenuation in air flow rate due to the length of tubes is neglected in the modeling. At the end, a model is proposed by combining these sub-models.

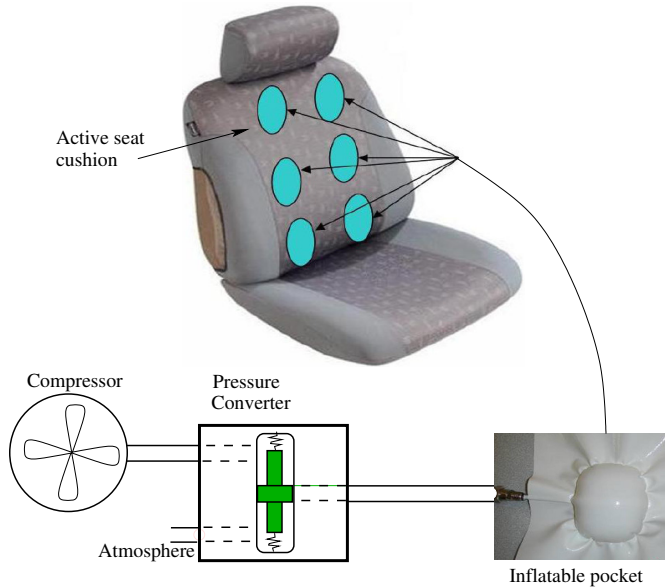


Fig. 1. An active inflatable seat

In order to model it, the mechanical equation of the spool valve is obtained from Newton's second law with all the forces acting on it:

$$m_p \ddot{x}_p = F_{mag} - (p_s - p_{atm})A_p - d_p \dot{x}_p - k_p x_p \quad (1)$$

where m_p , x_p , d_p and k_p are respectively, the plunger mass, the plunger position, its damping constant and spring constant, respectively. A_p and p_s are the spool valve area and the pressure inside the pocket, respectively. The magnetic force F_{mag} is given by the following equation:

$$F_{mag} = Du(t - \tau) \quad (2)$$

2.1 Pressure inside the ITP

The pressure inside the pocket is obtained by using the ideal gas equation. Here, the variation in temperature of the gas is assumed negligible:

$$p_s V_s = m_s R T_s \quad (3)$$

where p_s , V_s , m_s , R and T_s are respectively, the pressure inside the pocket, its volume, the amount of air mass inside it, the gas constant for air and the temperature inside. The pressure dynamics inside the ITP depends on its volume and flow of air into the pocket. Therefore, by taking the partial derivative, equation (3) can be written as:

$$\dot{p}_s = \frac{RT_s}{V_s} \dot{m}_s + m_s R T_s \left[\frac{-\dot{V}_s}{V_s^2} \right] \quad (4)$$

By using the ideal gas equation and simplifying above equation, the following equation is obtained:

$$\dot{p}_s = \frac{RT_s}{V_s} \dot{m}_s - \frac{p_s}{V_s} \dot{V}_s \quad (5)$$

Air mass flow: The air mass flow through a duct can be represented by the *Barré de Saint-Venant* equation which is used for compressible fluid flow. Indeed, the orifice of the proportional valve is considered as a duct (Heywood, 1988). The air can flow either from the ITP to atmosphere or from air pressure source to the ITP. The total amount of air mass flow to the pocket is the difference of air flowing in and out from it, hence, it can be expressed as follows:

$$\dot{m}_s = \dot{m}_{s-in} - \dot{m}_{s-out} \quad (6)$$

The equation of air flow rate from ITP and towards atmosphere \dot{m}_{s-out} is given by the following equation:

$$\dot{m}_{s-out} = A_{eff(s-atm)} p_s \sqrt{\frac{\gamma}{RT_s}} \Phi(p_r), \text{ with } p_r = \frac{p_s}{p_{atm}} \quad (7)$$

where $A_{eff(s-atm)}$ is the effective flow area between the pocket and the atmosphere. The function $\Phi(p_r)$ is an expression which depends on the upstream and the downstream pressure ratio p_r . Here, the upstream pressure is the pressure in the ITP (p_s) and downstream pressure is the atmospheric pressure (p_{atm}). The flow of air from source reservoir (a compressor) to the seat pocket \dot{m}_{s-in} is represented by the following equation:

$$\dot{m}_{s-in} = A_{eff(res-s)} p_{res} \sqrt{\frac{\gamma}{RT_{res}}} \Phi(p_r^*), \text{ with } p_r^* = \frac{p_{res}}{p_s} \quad (8)$$

Here, $A_{eff(res-s)}$ is the effective flow area of the valve between the seat pocket and the source reservoir. In this case, the upstream pressure is the pressure of the source (p_{res}) and the downstream pressure is the pressure of ITP (p_s). The pressure ratio p_r depends upon the amount of fluid mass which causes an increase in downstream pressure or drop in upstream pressure. When this ratio is less than or equal to 0.528, the fluid flow enters to supersonic from subsonic conditions (Heywood, 1988; Oosthuizen and Carscallen, 1997), and the amount of air flow becomes constant. The expression for subsonic and supersonic conditions is provided in the following equation (Heywood, 1988):

$$\Phi(p_r) = \begin{cases} \sqrt{\left\{ (p_r)^{2/\gamma} - (p_r)^{(\gamma+1)/\gamma} \right\} \frac{2}{\gamma-1}}, & p_r \geq \left(\frac{2}{\gamma+1} \right)^{\gamma/(\gamma-1)} \\ \sqrt{\left(\frac{2}{\gamma+1} \right)^{(\gamma+1)/2(\gamma-1)}}, & p_r < \left(\frac{2}{\gamma+1} \right)^{\gamma/(\gamma-1)} \end{cases} \quad (9)$$

The effective flow area A_{eff} is represented as a function of valve linear position x_1^* , with $x_1^* = 0.0504 - x_1$. The value of $x_1 = 0.0504$, corresponds to the intersection point where air flow reverses its direction. Hence,

$$A_{eff} = A_{eff(s-am)} = A_{eff(res-s)} = A_v x_1^*$$

Volume of the pocket: The volume of the pocket V_s varies with the amount of air entering in it. Thence, it is modeled and identified as a function of pressure. We have considered that the pocket has a perfect spherical shape. According to the theory of pressure vessels (Lee, 2008), (Fryer and Harvey, 1998), the hoop stress σ_θ and the longitudinal stress σ_a can be obtained using the following equation:

$$\sigma_\theta = \sigma_a = \frac{r(p_s - p_{atm})}{2s} \quad (10)$$

where r and s are, respectively, the radius of the sphere and the thickness of the fabric material. It is obvious that because of the spherical symmetry, both stresses are equal i.e. $\sigma_a = \sigma_\theta = \sigma$. The knowledge of the stresses allows us to calculate the elastic deformations and, consequently, variations in the dimensions of the pocket. The elastic deformation ε can, then, be expressed in terms of material characteristics using the following equation (Lee, 2008):

$$\varepsilon = \frac{1}{E} \sigma (1 - \nu) = \frac{r_{fin} - r_{in}}{r_{in}} \quad (11)$$

where E , ν , r_{fin} and r_{in} are, respectively, the Young modulus, the Poisson's ratio, the final and the initial values of radius of the sphere. Using the above equations, it is then possible to determine the final value of the radius of the sphere:

$$r_{fin} = r_{in} (1 + \varepsilon)$$

At this point, it is easy to understand how it is possible to express the variation of volume as a function of stress and elastic deformations (Fryer and Harvey, 1998):

$$\dot{V}_s = V_{fin} - V_{in} = \frac{4}{3} \pi (r_{fin}^3 - r_{in}^3) \quad (12)$$

Finally, by combining equations (1), (5), (6) and (12), the following nonlinear model of the ITP is proposed

$$\begin{aligned} \dot{x}_1 &= x_2 \\ \dot{x}_2 &= (F_{mag} - (x_3 - p_{atm})A_p - d_p x_2 - k_p x_1) / m_p \\ \dot{x}_3 &= \frac{\sqrt{\gamma R T_s}}{V_s} A_{eff} \left[\frac{x_3}{\sqrt{T_s}} \Phi(p_r) - \frac{p_{res}}{\sqrt{T_{res}}} \Phi(p_r^*) \right] - \frac{4\pi r^3}{3V_s} x_3 \end{aligned} \quad (13)$$

where x_1 , x_2 and x_3 are, respectively, the state variables for the spool valve position, its velocity and the pressure inside the pocket chamber.

3. CONTROL DESIGN

The goal of this section is to design a controller, based on the classical linear control theory. The control objective is to force the pressure converter, to reproduce the reference pressure trajectory. First, the model (13) is linearized to design after the PID control.

3.1 System linearization

The equation set (13) represents a nonlinear model of the EPC and the ITP. To linearize it around an operating point $P_1(x_{10}, x_{20}, x_{30})$, let's define three functions f_1 , f_2 and f_3 , such as:

$$\begin{aligned} f_1 &= x_2 \\ f_2 &= (Du - (x_3 - p_{atm})A_p - d_p x_2 - k_p x_1) / m_p \\ f_3 &= \frac{\sqrt{\gamma R T_s}}{V_s} A_v x_1^* \left[\frac{x_3}{\sqrt{T_s}} \Phi(p_r) - \frac{p_{res}}{\sqrt{T_{res}}} \Phi(p_r^*) \right] - \frac{4\pi r^3}{3V_s} x_3 \end{aligned} \quad (14)$$

Let's, also, consider the new states of the system (13) i.e. Δ_1 , Δ_2 and Δ_3 with input Δ_u and output Δ_3 , such that:

$$\begin{aligned} \Delta_1 &= x_1 - x_{10}, & \Delta_2 &= x_2 - x_{20}, & \Delta_3 &= x_3 - x_{30} \\ \Delta_u &= u - u_0, & y &= \Delta_3 = x_3 - x_{30} \end{aligned} \quad (15)$$

where x_{10} , x_{20} and x_{30} are the steady state values of the system at the chosen operating point P_1 and for the input u_0 . The elements of the linearized matrix A are obtained by taking the partial derivatives of functions f_i with respect to x_j such that

$$A_{ij} = \left. \frac{\partial f_i}{\partial x_j} \right|_{x_{j0}, u_0} \quad \text{for all } \{i, j\} = 1, 2, 3$$

$$\begin{aligned} A_{11} &= \left. \frac{\partial f_1}{\partial x_1} \right|_{x_{10}, u_0} = 0, & A_{12} &= \left. \frac{\partial f_1}{\partial x_2} \right|_{x_{20}, u_0} = 1 \\ A_{13} &= \left. \frac{\partial f_1}{\partial x_3} \right|_{x_{30}, u_0} = 0 \\ A_{21} &= \left. \frac{\partial f_2}{\partial x_1} \right|_{x_{10}, u_0} = -\frac{k_p}{m_p}, & A_{22} &= \left. \frac{\partial f_2}{\partial x_2} \right|_{x_{20}, u_0} = -\frac{d_p}{m_p} \\ A_{23} &= \left. \frac{\partial f_2}{\partial x_3} \right|_{x_{30}, u_0} = -\frac{A_p}{m_p} \\ A_{31} &= \left. \frac{\partial f_3}{\partial x_1} \right|_{x_{10}, u_0} = \frac{\sqrt{\gamma R}}{V_s} T_s A_v \left(\frac{p_{res}}{\sqrt{T_{res}}} \varphi(p_r^*) - \frac{x_{30}}{\sqrt{T_s}} \varphi(p_r) \right) \\ A_{32} &= \left. \frac{\partial f_3}{\partial x_2} \right|_{x_{20}, u_0} = 0 \\ A_{33} &= \left. \frac{\partial f_3}{\partial x_3} \right|_{x_{30}, u_0} = -\frac{\sqrt{\gamma R T_s}}{V_s} A_v x_{10} \varphi(p_r) - \frac{4\pi r^3}{3V_s} \end{aligned} \quad (16)$$

The matrix B for a single input single output (SISO) system is defined as, $B_{i1} = \frac{\partial f_i}{\partial u}$ for all $i = 1, 2, 3$

$$B_{11} = \frac{\partial f_1}{\partial u} = 0, \quad B_{21} = \frac{\partial f_2}{\partial u} = \frac{D}{m_p}, \quad B_{31} = \frac{\partial f_3}{\partial u} = 0 \quad (17)$$

Hence, the state space model, obtained after linearizing the system (13), is given below:

$$\begin{bmatrix} \dot{\Delta}_1 \\ \dot{\Delta}_2 \\ \dot{\Delta}_3 \end{bmatrix} = \begin{bmatrix} A_{11} & A_{12} & A_{13} \\ A_{21} & A_{22} & A_{23} \\ A_{31} & A_{32} & A_{33} \end{bmatrix} \begin{bmatrix} \Delta_1 \\ \Delta_2 \\ \Delta_3 \end{bmatrix} + \begin{bmatrix} B_{11} \\ B_{21} \\ B_{31} \end{bmatrix} \Delta_u \quad (18)$$

The linearized state space model can be also represented by the following transfer function:

$$T_r(s) = \frac{9.08 \times 10^4 s^2 + 3.5 \times 10^7 s + 5.81 \times 10^8}{s^3 + 516.5s^2 + 5.7 \times 10^4 s + 8.4 \times 10^5} \quad (19)$$

where T_r is the transfer function between the output Δ_3 and the input Δ_u .

3.2 Control requirements

To achieve the desired steady state and transient response of the system, the design requirements for the controller are set as given below:

- Rise time = 0.5 sec
- Setting time = 2 sec
- Maximum overshoot = 10 %

The final proposed PID controller satisfying the above mentioned requirements is given:

$$C(s) = 0.0689 \left(\frac{1 + 1.09s + 0.02s^2}{s} \right) \quad (20)$$

In Fig. 2, Root Locus and open-loop Bode plot of the system (19) are shown with the designed PID controller given by equation (20). The phase crossover frequency is at 78.4 rad/sec , while the gain crossover frequency is at 0 rad/sec . The system is closed loop stable with the stability margins $GM = -361 \text{ dB}$ and $PM = 57.3^\circ$.

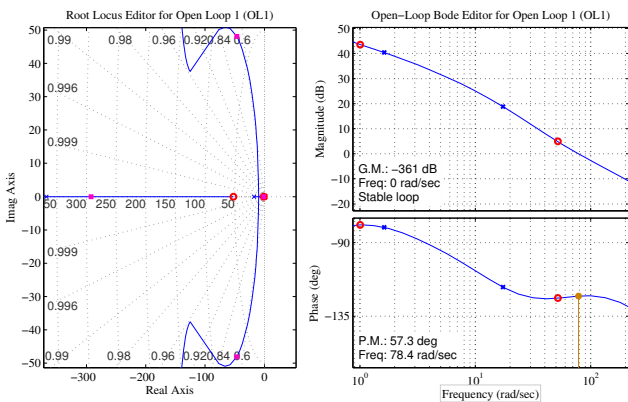


Fig. 2. Designing a PID controller with sisotool program of Matlab

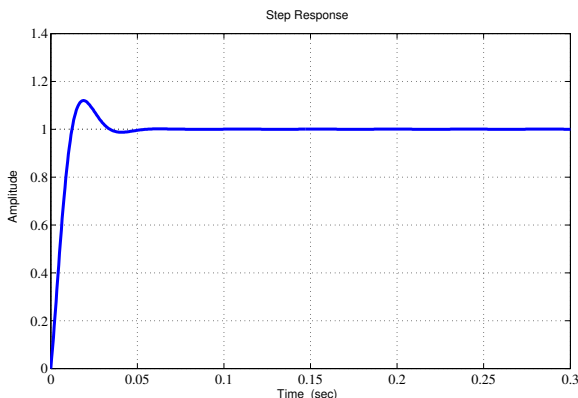


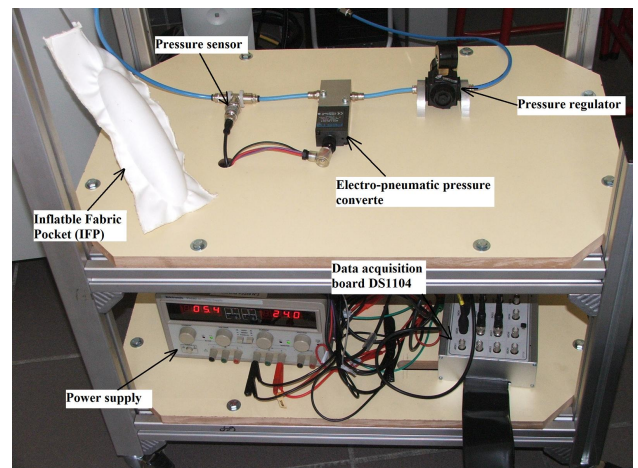
Fig. 3. Step response of the system with controller by using design constraints

Therefore, by applying the control law (20) on the linear model (19), with design parameters given above, we get the step response of the feedback system as given in Fig. 3. Let us

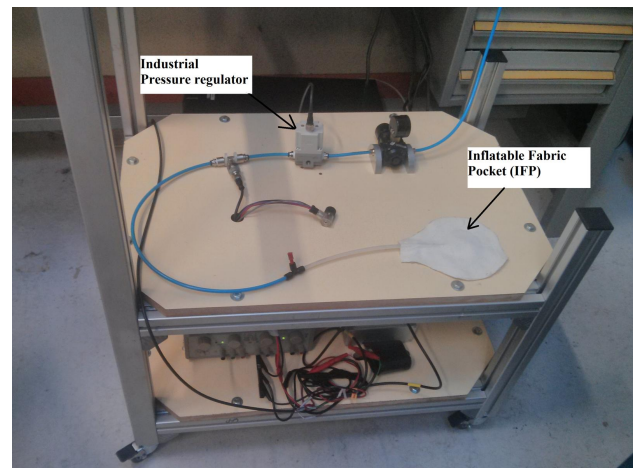
emphasize that the pure derivative action in (20) is replaced in practice by a lead phase approximation to obtain a causal controller.

4. EXPERIMENTAL VALIDATION

The following section briefly shows the instrumentation used for the control analysis of the textile pocket. The developed experimental test bench consists of data acquisition system (a Dspace® DS1104 controller board), a power supply, a pressure converter, a pressure sensor and an ITP. The pressure converter is a proportional valve Festo MPYE-5-M5-010-B which works with the controlled voltage applied through Dspace® board and it varies from 0 to 10 volts. The pressure source, applied to the system, is regulated via a manual pressure regulator. Fig. 4(a) shows the complete experimental test bench with Electro-pneumatic Festo Pressure Converter. To compare the performance of the pressure converter, another industrial regulator SMC(ITV1000 series) is used in place of pressure converter as shown in Fig. 4(b).



(a) Experiments performed with an Electro-pneumatic Pressure Converter



(b) Experiments performed with an industrial pressure regulator

Fig. 4. Test bench for experiments

4.1 Sine reference tracking

Firstly, the test bench shown in Fig. 4(a) is used to validate the proposed PID controller for a desired pressure signal. The

desired pressure signal is a sine wave with frequency of 0.16 Hz and amplitude of 40 kPa [*i.e.* 120 kPa (absolute) $\pm 20\text{ kPa}$]. Then, the EPC is replaced with an industrial pressure regulator as shown in Fig. 4(b). In Fig. 5, both the output signal are shown along with the desired pressure signal inside the ITP. Whereas, the error between desired and both the output signals, obtained from two different pressure converters, are shown in Fig. 6. It can be seen that this error is 3.125 times higher when the industrial pressure regulator is used instead of the proposed control law.

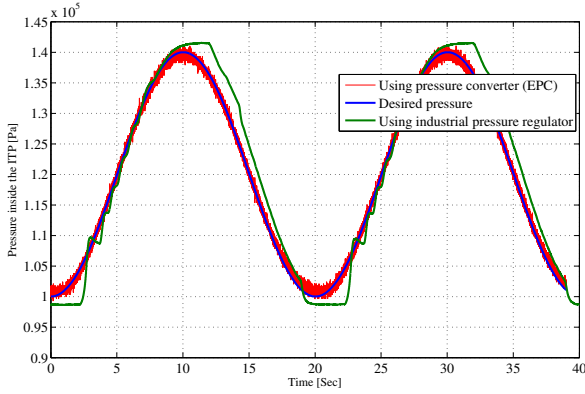


Fig. 5. Pressure tracking inside an ITP (sine wave)

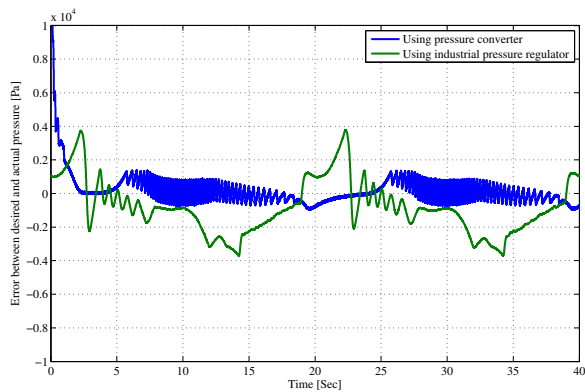


Fig. 6. Error between the reference pressure and the actual pressure of sine wave

4.2 Step reference tracking

Similarly, a step reference trajectory is tested on both the test benches shown in Fig. 4. The desired pressure signal is a step with amplitude of 20 kPa . The initial absolute pressure is 100 kPa . The desired pressure signal along with both the signal obtained from two different pressure regulators, are shown in Fig. 7. It can be seen that the error for industrial regulator never reaches to zero (see Fig. 8).

Furthermore, robustness of the controller is tested by applying external disturbance forces. The latter are applied randomly to the ITP. The results provided in Fig. 9 show that the proposed EPC based pressure regulator is robust, while the industrial regulator does not support the sudden changes in the actual pressure. Fig. 10 shows the error signal between the desired pressure and the actual pressure for both the proposed EPC and the industrial pressure regulator.

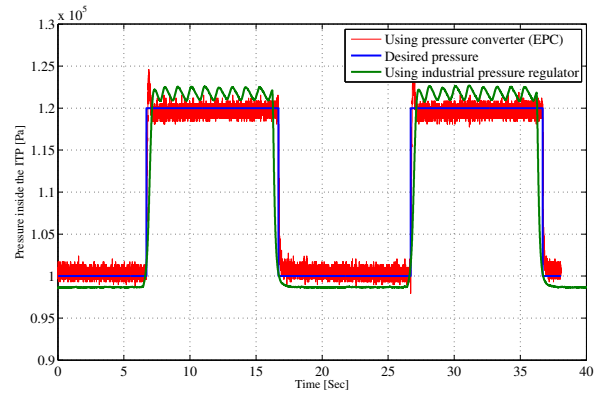


Fig. 7. Pressure tracking inside an ITP (step signal)

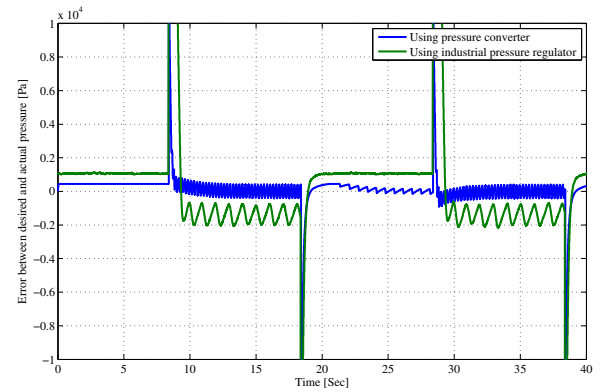


Fig. 8. Error between the reference pressure and the actual pressure of step signal

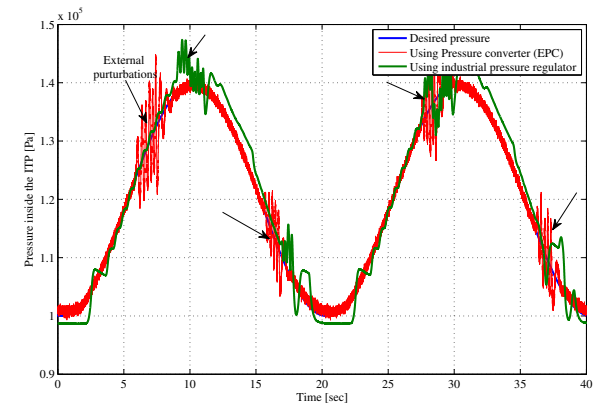


Fig. 9. Pressure tracking inside an ITP with perturbation forces (sine wave)

From the response of both the pressure converters, it can be concluded that the proposed control law using an EPC provides better results. This comparison is summarised in Table. 1 along with other factors.

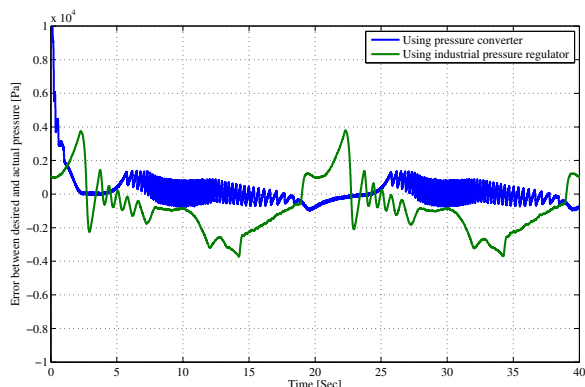


Fig. 10. Error between the reference pressure and the actual pressure of sine wave with disturbance forces

Table 1. Comparison between the EPC and an industrial pressure regulator

Property	Pressure converter (EPC)	Industrial Pressure regulator
Type of solenoid valve	Proportional	On/Off
Number of ports	5	3
Embedded controller	No	Yes
Feedback	Valve position	Air pressure
Price	510 €	380 €
Output error	$\pm 800Pa$	$\pm 2500Pa$

5. CONCLUSION

In this article, a new control oriented nonlinear model of an Inflatable textile Textile Pocket (ITP) has been presented. These textile pockets will be integrated into driver's seat to obtain an adjustable backrest. The system consists of a pressure source, a pressure converter and an inflatable pocket. The complete model of this system is linearized around an operating point for control analysis and implementation. As a first step, a PID control is implemented on an experimental test bench developed in the lab. The performance of the proposed PID controller is then compared with an industrial pressure regulator. The developed test bench along with PID controller shows better transient and steady state responses. To improve the performance of the feedback system, more sophisticated control techniques will be implemented on the test bench.

REFERENCES

Alali, M. (2008). Conception d'une machine de fatigue: test de poches complexes tissées (french). *Masters thesis, Université de Haute-Alsace, France*.

Bialkowski, W.L. (1996). Control of the pulp and paper making process. *The Control Handbook IEEE Press*.

Canudas de Wit, C., Olsson, H., Astrom, J.K., and Lischinsky, P. (1995). A new model for control of systems with friction. *IEEE Transactions on Automatic Control*, 40(3), 419–426.

Chawla, A., Bhosale, P.V., and Mukherjee, S. (2005). Modeling of folding of passenger side airbag mesh. *SAE technical paper*, (2005-26-059).

Fryer, D.M. and Harvey, J.F. (1998). *High pressure vessels*. Publishers Chapman and Hall, ISBN-13: 978-0412074516.

Gulati, N. and Barth, E.J. (2007). Dynamic modeling of a monopropellant-based chemofluidic actuation system. *Journal of dynamic systems measurement and control*, 129, 435–445.

Heywood, J. (1988). *Internal Combustion Engine Fundamentals*. Publishers McGraw-Hill, ISBN-13: 978-0070286375.

Lee, D.W. (2008). An innovative inflatable morphing body structure for crashworthiness of military and commercial vehicles. *PhD thesis, University of Michigan, USA*.

Olaby, O., Brun, X., Semat, S., Redarce, T., and Bideaux, E. (2005). Characterization and modeling of a proportional valve for control synthesis. *In Proc. 6th JFPS symposium on Fluid Power, Tsukuba, Japan*.

Oosthuizen, P. and Carscallen, W. (1997). *Compressible Fluid Flow*. Publishers McGraw-Hill, ISBN-13: 978-0070481978.

Rangnath, D.G. (2009). Modeling and analysis of an inflatable lap belt airbag restraint system for frontal crash protection of mass transit bus operators. *Masters thesis, Wichita State University, USA*.

Rao, Z. and Bone, G. (2008). Nonlinear modeling and control of servo pneumatic actuators. *IEEE transactions on control systems technology*, 16(3), 562–569.

Silva, G.J., Datta, A., and Bhattacharyya, S.P. (2002). New results on the synthesis of pid controllers. *IEEE transactions on automatic control*, 47(2).

Smaoui, M., Brun, X., and Thomasset, D. (2007). High-order sliding mode for an electropneumatic system: A robust differentiator-controller design. *International journal of robust and nonlinear control*, 18, 481–501.

Taghizadeh, M., Ghaffari, A., and Najafi, F. (2009). Modelling and identification of a solenoid valve for pwm control applications. *Comptes Rendus Mecanique, Transactions of the Elsevier masson*, 337, 131–140.

Tulemat, M.A. (2007). Etude de poches tissées complexes gonflables: Application automobile. *Phd thesis (French), Université de Haute-Alsace, France*.

Wang, X., Cheng, Y., and Peng, G. (2007). Modeling and self tuning pressure regulator design for pneumatic-pressure load systems. *Journal of dynamic systems, measurement and control*, 15(9), 1161–1168.

Wickramatunge, K.C. and Leephakpreeda, T. (2013). Empirical modeling of dynamic behaviors of pneumatic artificial muscle actuators. *ISA Transactions, In press*, <http://dx.doi.org/10.1016/j.isatra.2013.06.009>.

Zhang, J., Lv, C., Yue, X., Li, Y., and Yuan, Y. (2013). Study on a linear relationship between limited pressure difference and coil current of on/off valve and its influential factors. *ISA Transactions, In press*, <http://dx.doi.org/10.1016/j.isatra.2013.09.008>.

Zilic, T., Pavkovic, D., and Zorc, D. (2009). Modeling and control of a pneumatically actuated inverted pendulum. *ISA Transactions*, 48, 327–335.